

# MiTA Attention: Efficient Fast-Weight Scaling via a Mixture of Top- $k$ Activations

Qishuai Wen<sup>1</sup> Zhiyuan Huang<sup>1</sup> Xianghan Meng<sup>1</sup> Wei He<sup>1</sup> Chun-Guang Li<sup>1</sup>

## Abstract

The attention operator in Transformers can be viewed as a two-layer *fast-weight MLP*, whose weights are dynamically instantiated from input tokens and whose width equals sequence length  $N$ . As the context extends, the expressive capacity of such an  $N$ -width MLP increases, but scaling its fast weights becomes prohibitively expensive for extremely long sequences. Recently, this *fast-weight scaling* perspective has motivated the Mixture-of-Experts (MoE) attention, which partitions the sequence into *fast-weight experts* and sparsely routes the tokens to them. In this paper, we elevate this perspective to a unifying framework for a wide range of efficient attention methods by interpreting them as scaling fast weights through either routing or compression. Then we propose a compress-and-route strategy, which compresses the  $N$ -width MLP into a narrower one using a small set of *landmark queries* and constructs *deformable experts* by gathering top- $k$  activated key-value pairs for each landmark query. We call this strategy a *Mixture of Top- $k$  Activations (MiTA)*, and refer to the resulting efficient mechanism as *MiTA attention*. Preliminary experiments on vision tasks demonstrate the promise of our MiTA attention and motivate further investigation on its optimization and broader applications in more challenging settings. Code is available at [this URL](#).

## 1. Introduction

Attention is the core operation of Transformers, which underpins today’s success and wide application of deep learning. Intuitively, attention learns to store the context as key-value associations and retrieve this short-term memory via queries (Bietti et al., 2023). However, such an all-to-all

<sup>1</sup>School of Artificial Intelligence, Beijing University of Posts and Telecommunications, Beijing, China. Correspondence to: Chun-Guang Li <lichunguang@bupt.edu.cn>.

Preprint. March 6, 2026.

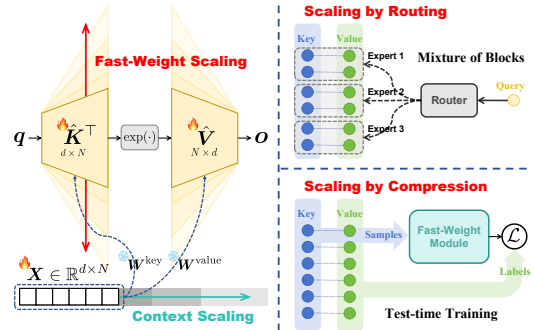


Figure 1. Fast-weight scaling and its two scaling strategies. As the context extends, the width of the two-layer fast-weight MLP induced by full attention increases accordingly. We categorize efficient fast-weight scaling approaches into two strategies: a) scaling by routing and b) scaling by compression, and illustrate each of them with a representative method: Mixture of Block Attention (MoBA) (Lu et al., 2025) and Test-time Training (TTT) (Sun et al., 2025). A pioneering method that combines both strategies is Native Sparse Attention (NSA) (Yuan et al., 2025).

lookup paradigm incurs quadratic computation and memory complexity in the sequence length, thereby hindering its scaling to long sequences. To this end, a plethora of efficient attention methods have been explored (Zhang et al., 2025).

In recent years, several lines of work have converged on a unifying viewpoint: *the key-value pairs in full attention can be viewed as the fast weights of an MLP (Schlag et al., 2021; Han et al., 2025); and the parameters of a two-layer MLP can be viewed as slow-weight key-value pairs (Geva et al., 2021)*. Therefore, pursuing an efficient attention can be framed as a *fast-weight scaling* problem, and draw inspiration from slow-weight (i.e., parameter) scaling approaches, such as weight tying (Wu et al., 2025a), model pruning (Cheng et al., 2024), and conditional computation (Riquelme et al., 2021).

Recent work along this direction has demonstrated that sparse attention inspired by Mixture-of-Experts (MoE) can scale up the effective sequence length, deliver wall-clock speedups, and accommodate large-scale pretraining (Lu et al., 2025; Yuan et al., 2025). In contrast to traditional MoE, whose experts are structured, input-independent model parameters (i.e., slow weights), their experts are input-dependent fast weights (Schmidhuber, 1992), more precisely, subsets of key-value pairs. Routing each query to

the fast-weight experts sparsely, MoE attention reduces the complexity from quadratic to linear in sequence length  $N$ .

Roughly speaking, the central challenge in scaling the fast weights via MoE is to construct fast-weight experts from unstructured key-value pairs. For example, given the spatial and temporal locality priors in many modalities, a straightforward, hardware-friendly approach is to partition the sequence into contiguous, non-overlapping, fixed-size blocks, and regard these blocks as fast-weight experts (i.e., a mixture of blocks or chunks) (Lu et al., 2025; Yuan et al., 2025; Wu et al., 2025b; Cai et al., 2025). After that, routing vectors are obtained by aggregating each block into a single vector, e.g., via average pooling or parameterized modules.

Since splitting the  $N$ -width fast-weight MLP into a mixture of such blocks is coarse and suboptimal, subsequent work (Jia et al., 2025) has sought to improve upon the splitting scheme. Notably, top- $k$  attention (You et al., 2025; Liu et al., 2025) can be interpreted as spawning  $N$   $k$ -width sub-MLPs (i.e., experts) from the  $N$ -width MLP, via gathering top- $k$  key-value pairs attended (i.e., activated) by each query. Therefore, the fixed-shape expert in prior MoE attention methods are replaced by top- $k$  attention with *deformable experts*. However, instead of the width of the fast-weight MLP in full attention, it is the number of such deformable fast-weight experts that always equals  $N$  in their top- $k$  attention.

On the other hand, unlike the above methods that scale fast weights by accessing a subset of them, linear attention (Katharopoulos et al., 2020) and Test-Time Training (TTT) (Sun et al., 2025) compress the  $N$ -width MLP into one (or several (Zhang et al., 2026)) light-weight module(s), analogous to model compression (Ba & Caruana, 2014) and knowledge distillation (Hinton et al., 2015). Therefore, from a fast-weight scaling perspective, we divide the scaling approaches of existing efficient attention methods discussed in this paper into two general categories: a) scaling by routing, and b) scaling by compression (see Fig. 1 for an illustration). Scaling by compression alone sacrifices a precise access to the original key-value pairs; whereas scaling by routing alone lacks a global summary of the full context. Although these two approaches are *not* mutually exclusive, most existing methods typically adopt only one of them.

In this paper, we elevate the fast-weight scaling perspective into a five-dimensional taxonomy that accommodates a broad spectrum of prior efficient-attention methods (see Tab. 1). While such a taxonomy is by no means complete, it paves the way towards a unified framework. Then, we propose to combine the two scaling strategies together and construct a tunable number of deformable fast-weight experts via **Mixture of Top- $k$  Activations (MiTA)**, which uses a small number of *landmark queries* to look up key-value pairs. Specifically, MiTA compresses the values as *land-*

*mark values*, yielding a compact key-value set (i.e., a narrower MLP) as a shared expert, in which landmark queries serve as compressed keys and landmark values serve as compressed values; and reorganizes the original key-value pairs into deformable routed experts via gathering top- $k$  key-value pairs activated by each landmark query. As shown in Fig. 2, MiTA attention concatenates these compressed key-value pairs with a routed, deformable subset of the original key-value pairs for each query.

**Contributions.** Contributions of the paper are summarized as follows.

1. We introduce a five-dimensional taxonomy to sort the existing efficient attention methods from a fast-weight scaling perspective.
2. We propose an efficient attention method—MiTA, which constructs a tunable number of deformable experts and combines the scaling-by-routing and scaling-by-compression strategies together.

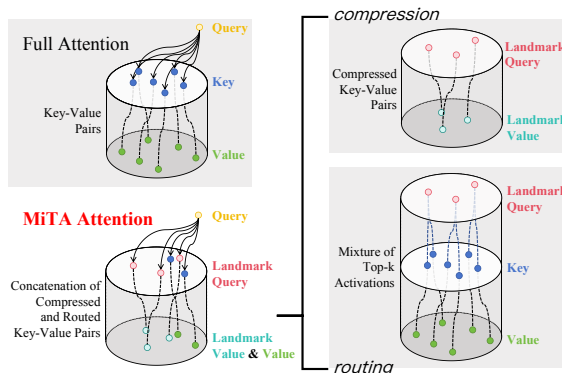


Figure 2. Illustration for our MiTA attention. In full attention, each query attends to all key-value pairs. In our MiTA attention, it attends to the concatenation of a small number (e.g., 3 as shown above) of the compressed key-value pairs and a routed subset of the full key-value pairs (2 above).

## 2. Related Work

### 2.1. Fast-Weight Scaling

In contrast to slow weights (i.e., model parameters) encoding persistent knowledge, fast weights are input-conditioned and can be viewed as short-term memory (Behrouz et al., 2024), playing an important role in meta-learning (Kirsch et al., 2022) and in-context learning (Chan et al., 2022). While most scaling efforts have focused on expanding slow weights (e.g., increasing model width and depth) (Kaplan et al., 2020; Tan & Le, 2019), extending Transformers’ sequence length turns out to implicitly scale fast weights.

For instance, Test-Time Training (TTT) (Sun et al., 2025) effectively compresses the  $N$ -width two-layer fast-weight MLP in full attention into a smaller fast-weight module, like-

Table 1. A five-dimensional taxonomy for efficient attention methods from the fast-weight scaling perspective. We present expert type and expert count together in the table. The analysis of this taxonomy and how MiTA Attention fits into it can be found in Sec. 3.3.

Method	Scaling strategy	Expert type and count	Expert construction	Routing topology
Linear Attention (2020) MHLA (Zhang et al., 2026)	Compression	One shared linear layer $m$ linear layers	Kernelization Local prior & kernelization	All-to-one $m$ times $\frac{N}{m}$ -to-one
Linformer (Wang et al., 2020) PVT (Wang et al., 2021)	Compression	One shared MLP	Learnable projection	All-to-one
Agent Attention (Han et al., 2024b)	Compression	One shared MLP	Landmark probing	All-to-one
TTT (Sun et al., 2025) ViT <sup>3</sup> (Han et al., 2025)	Compression	One shared module	Test-time training	All-to-one
Deformable DETR (2017) DAT (Xia et al., 2022)	Routing	$N$ MLPs One shared MLP	Offset predicting	$N$ times one-to-one $N$ -to-one
BRA (Zhu et al., 2023) MoBA (Lu et al., 2025) NSA (Yuan et al., 2025)	Routing Routing Compression & Routing	$\frac{N}{n}$ MLPs	Locality prior	$\frac{N}{n}$ -to- $\frac{N}{n}$ $N$ -to- $\frac{N}{n}$
Spark Attention (You et al., 2025) DSA (Liu et al., 2025)	Routing	$N$ MLPs	Light-weight skim	$N$ times one-to-one
<b>MiTA Attention (ours)</b>	Compression & Routing	$m$ MLPs	Landmark probing	$N$ -to- $m$

wise for linear attention (Katharopoulos et al., 2020) into a linear layer (Han et al., 2025) and Linformer (Wang et al., 2020) into a narrower MLP. Rather than scaling by compressing the full fast-weight MLP, MoE attention factorizes it into experts and access them sparsely via routing.

In our MiTA, the two strategies mentioned above—scaling by compressing and scaling by sparse routing—are combined. It follows the Agent Attention (Han et al., 2024b) to compress full key-value pairs into a smaller set (i.e., a narrower MLP), which offers a coarse yet global summary, and then leverages the top- $k$  activations of the agent tokens (i.e., landmark queries) to identify underlying experts, which enables precise retrieval.

## 2.2. MoE-Inspired Sparse Attention

Previous sparse attention methods typically focus on the design of fixed sparse patterns (e.g., the local window, axial stripe (Dong et al., 2022), and the vertical-slash pattern (Jiang et al., 2024)) or learnable ones (e.g., hash buckets (Kitaev et al., 2020) and  $k$ -means clusters (Roy et al., 2021).) To maintain a global connectivity, shared memory (i.e., tokens that attend to and are attended by all tokens) is also introduced (Beltagy et al., 2020). However, these patterns are either task-dependent (Lai et al., 2025) or too burdensome to achieve wall-clock speedup (Dao et al., 2022).

Recently, sparse attention inspired by Mixture-of-Experts (MoE) has been applied to pre-training large language models, yielding extended effective context with reduced overhead (Lu et al., 2025; Yuan et al., 2025). Its key advantage is the routing mechanism, which enables query-aware selection within the key-value cache. Consequently, de-

spite coarse selection granularity (e.g., evenly split, non-overlapping blocks), the sparse pattern is highly flexible and can vary across queries.

In this paper, we argue that, beyond routing, the experts can also be query-aware and deformable. Specifically, for an arbitrarily long sequence, we can build a fixed, yet configurable number of experts by gathering semantically related key-value pairs. A similarly motivated line of research is to replace the fixed, non-overlapping rectangular patchification in ViTs (Dosovitskiy et al., 2021) with a deformable, content-adaptive tokenization scheme (Chen et al., 2021b).

## 2.3. Deformable Attention

More broadly, conditional computation, the idea underlying MoE, has been explored through the deformable convolution (Dai et al., 2017) in convolutional neural networks. And deformable attention was introduced for object detection by Zhu et al. (2021) and later generalized to Vision Transformers by Xia et al. (2022). Given a query, while being blind to keys, deformable attention predicts offsets relative to a small set of default positions of the keys, thereby inducing a query-aware, deformable sparse attention pattern (i.e., a fast-weight expert in our context).

Recent top- $k$  attention methods, e.g., Spark Attention (You et al., 2025) and DeepSeek Sparse Attention (Liu et al., 2025), which have been applied to the training of Gemma 3n and DeepSeek-V3.2, respectively, can also be viewed as improved deformable attention. Instead of predicting the spatial positions solely from the query as in prior deformable attention, these methods locate the top- $k$  key-value pairs by allowing each query to take a lightweight skim of the full keys, e.g., using partial features (You et al., 2025) or

low precision (FP8) (Liu et al., 2025). Our MiTA retains the key advantage of the top- $k$  attention by constructing deformable experts (i.e., sparse patterns) that depend on both queries and keys. However, unlike the deformable attention methods discussed above, we replace the per-query offset predicting (Zhu et al., 2021; Xia et al., 2022) or light-weight skim (You et al., 2025; Liu et al., 2025) with more efficient per-query routing.

### 3. Methods

#### 3.1. Efficient Attention as Fast-Weight Scaling

This subsection will first present the mathematical formulation of the fast-weight MLP in full attention, and then reinterpret efficient attention as a fast-weight scaling problem. From this perspective, a taxonomy of previous efficient attention methods in terms of how they scale fast weights will be given.

**Fast-weight MLP.** Formally, full attention (i.e., scaled dot-product attention (Vaswani et al., 2017)) can be written as:

$$\text{Atten}(\mathbf{q}, \mathbf{K}, \mathbf{V}) = \mathbf{V} \text{softmax}\left(\frac{\mathbf{K}^\top \mathbf{q}}{\sqrt{d}}\right), \quad (1)$$

where  $\mathbf{q} \in \mathbb{R}^d$  is a query, and the columns of  $\mathbf{K}, \mathbf{V} \in \mathbb{R}^{d \times N}$  are the keys and values, respectively. By contrast, a  $D$ -width two-layer MLP, i.e., the feed-forward network (FFN) in Transformers, is:

$$\text{MLP}_\sigma(\mathbf{x} \mid \mathbf{W}_1; \mathbf{W}_2) = \mathbf{W}_2 \sigma\left(\mathbf{W}_1^\top \mathbf{x} + \mathbf{b}_1\right) + \mathbf{b}_2, \quad (2)$$

where  $\mathbf{x} \in \mathbb{R}^d$  is the input vector,  $\mathbf{W}_1, \mathbf{W}_2 \in \mathbb{R}^{d \times D}$  are weights,  $\mathbf{b}_1 \in \mathbb{R}^D$  and  $\mathbf{b}_2 \in \mathbb{R}^d$  are biases<sup>1</sup>, and  $\sigma(\cdot)$  is an element-wise activation function (e.g., ReLU). Note that full attention in Eq. (1) is equivalent to the following MLP:

$$\text{MLP}_{\text{exp}}(\mathbf{q} \mid \hat{\mathbf{K}}; \hat{\mathbf{V}}) = \hat{\mathbf{V}} \exp\left(\hat{\mathbf{K}}^\top \mathbf{q}\right), \quad (3)$$

$$\hat{\mathbf{K}} = \mathbf{K}/\sqrt{d}, \quad \hat{\mathbf{V}} = \mathbf{V} / \left(\exp(\hat{\mathbf{K}}^\top \mathbf{q})^\top \mathbf{1}_N\right), \quad (4)$$

where the weights are given by the scaled keys and values, the biases are all zero, and the activation function is the exponential function  $\exp(\cdot)$ . Therefore, we have demonstrated that full attention in Eq. (1) is equivalent to the  $N$ -width, fast-weight, two-layer MLP in Eq. (3).

**Unbounded fast-weight scaling.** Because the hidden dimension of the fast-weight MLP in Eq. (3) always equals to the sequence length  $N$ , the per-query overhead grows linearly with  $N$  rather than fixed as in the slow-weight MLP in Eq. (2). Thus, under the all-to-all lookup paradigm, processing  $N$  queries incurs an overall  $\mathcal{O}(N^2)$  overhead. This unbounded, rapid growth prevents scaling the fast weights

<sup>1</sup>For notion simplicity, biases are omitted from the argument.

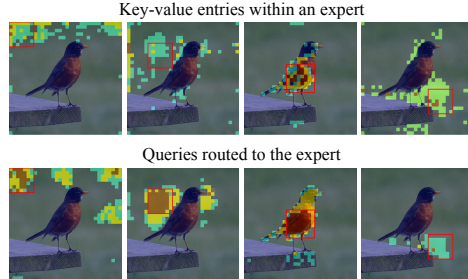


Figure 3. Visualization of experts’ gathered key-value pairs, and routed queries. The red box marks the local window from which the landmark query is obtained via average pooling. The attention heatmap (averaged over attention heads) indicates key-value pairs within each expert (top row) and the queries routed to it (bottom row). Notably, neither the expert’s key-value pairs nor the routed queries are confined to the local window.

to arbitrarily long sequences. While this challenge is commonly described as the quadratic complexity of full attention in the literature on efficient attention, we refer to it as the *unbounded fast-weight scaling* issue.

**Fast-weight scaling taxonomy.** Although we have discussed relevant efficient-attention methods in Sec. 2, they have not been systematically organized into a unified fast-weight scaling perspective. We therefore propose a five-dimensional taxonomy: a) *scaling strategy*, i.e., scaling the  $N$ -width fast-weight MLP either by compressing it into a light-weight module or by routing each query to a subset of it; b) *expert count*, i.e., how many fast-weight experts are constructed (in particular, scaling by compression typically yields a single shared expert); c) *expert type*, i.e., what module each expert takes (e.g., an MLP or a linear layer); d) *expert construction*, i.e., how experts are formed from the key-value pairs; and e) *routing topology*, i.e., the query-expert assignment pattern. The mapping of existing methods to this taxonomy is summarized in Tab. 1. We defer the in-depth discussion until Sec. 3.3.

#### 3.2. Mixture of Top- $k$ Activations (MiTA) and MiTA Attention

Both scaling by compression and scaling by routing have inherent limitations. Compressing the full fast-weight MLP inevitably discards information, although the information loss can be mitigated by adopting milder compression schemes (e.g., piecewise compression (Zhang et al., 2026)) or by compressing into a more expressive module (e.g., via test-time training (Sun et al., 2025)). In contrast, scaling by routing is faithful and lossless, but it often lacks a global view of the context.

To combine the strengths of both strategies, i.e., to retain a compact global summary while enabling precise, token-level retrieval, we introduce a small set of *landmark queries*  $\tilde{\mathbf{Q}} \in \mathbb{R}^{d \times m}$  with  $m \ll N$ . These landmark queries probe the full key-value cache and then, via cross-attention, com-

press it into a global fast-weight module, while simultaneously forming deformable fast-weight experts by gathering the top- $k$  activated key-value pairs for each landmark query.

This design is motivated by two observations: a) register tokens can attend to distinct semantic regions (i.e., fast-weight experts) of an image (Darcet et al., 2024); and b) class embeddings (Strudel et al., 2021) (or object queries (Carion et al., 2020) and mask embeddings (Cheng et al., 2021)) provide a compact global summary for dense prediction tasks (Wen & Li, 2024) and even image generation (Yu et al., 2024). The landmark queries can be obtained in various ways, e.g., by assigning a set of learnable slow weights or by downsampling the sequence using a convolutional module. In this work, we simply apply average pooling over uniformly spaced, equal-sized windows, as shown in Fig. 3.

Specifically, the  $i$ -th landmark query  $\tilde{q}_i$  defines the  $i$ -th expert  $\mathcal{E}_i$  as follows:

$$\mathcal{E}_i(\mathbf{q}) = \text{Atten}(\mathbf{q}, \mathbf{K}^{(i)}, \mathbf{V}^{(i)}), \quad i \in \{1, \dots, m\}, \quad (5)$$

$$\mathbf{K}^{(i)} = \mathbf{K}_{:, \mathcal{I}_i}, \quad \mathbf{V}^{(i)} = \mathbf{V}_{:, \mathcal{I}_i} \in \mathbb{R}^{d \times k}, \quad (6)$$

$$\mathcal{I}_i = \text{Top}_k(\mathbf{K}^\top \tilde{\mathbf{q}}_i) \in \{1, \dots, N\}^k, \quad (7)$$

where  $\mathbf{q}$  is a query routed to expert  $\mathcal{E}_i$ , and  $\mathbf{K}^{(i)}, \mathbf{V}^{(i)}$  are the top- $k$  key-value pairs activated by  $\tilde{\mathbf{q}}_i$ . This approach effectively reorganizes the full key-value pairs into a **Mixture of Top- $k$  Activations (MiTA)** (i.e., a mixture of deformable experts). We directly use  $\tilde{\mathbf{q}}_i$  as the routing vector for expert  $\mathcal{E}_i$ . Then the routing logits from the  $N$  queries  $\mathbf{Q} \in \mathbb{R}^{d \times N}$  to the  $m$  experts is  $\mathbf{Q}^\top \tilde{\mathbf{Q}} \in \mathbb{R}^{N \times m}$ . We denote the index of the rank- $j$  expert that a query  $\mathbf{q}$  is routed to under these logits as  $e_j(\mathbf{q}) \in \{1, \dots, m\}$ .

Moreover, regarding the compressed global module, which can be viewed as a shared expert (Dai et al., 2024), we extract a set of *landmark values*  $\tilde{\mathbf{V}} \in \mathbb{R}^{d \times m}$  via cross-attention using the landmark queries. The  $i$ -th landmark value corresponding to the  $i$ -th landmark query is given by:

$$\tilde{v}_i = \text{Atten}(\tilde{\mathbf{q}}_i, \mathbf{K}, \mathbf{V}). \quad (8)$$

Then, the shared expert  $\tilde{\mathcal{E}}$  is defined as:

$$\tilde{\mathcal{E}}(\mathbf{q}) = \text{Atten}(\mathbf{q}, \tilde{\mathbf{Q}}, \tilde{\mathbf{V}}), \quad (9)$$

where landmark queries act as the keys in standard attention. Note that the computations in Eqs. (7) and (8) can be largely shared, where landmark queries are both querying the keys. Likewise, Eq. (9) can reuse the routing logits. Therefore, the computations of the two scaling strategies are tightly coupled in our MiTA.

Rather than a straightforward MoE implementation, which isolates the computation within each expert and aggregates their outputs via a weighted sum, we concatenate the experts

---

**Algorithm 1** Mixture of Top- $k$  Activations (MiTA) attention
 

---

**Require:** Query, key, value matrices  $\mathbf{Q}, \mathbf{K}, \mathbf{V} \in \mathbb{R}^{d \times N}$ ; the number of landmark queries  $m$ ; the width of each fast-weight expert  $k$ ; each query is routed to the shared expert and to  $s = 1$  additional expert.

```

1: // Obtain landmark queries
2:  $\tilde{\mathbf{Q}} = \text{AdaptiveAvgPool}(\mathbf{Q}, \text{output\_size}=m)$  // [d, m]
3: // Lookup key-value pairs via landmark queries
4:  $\mathbf{S}^{\text{kv}} = \mathbf{K}^\top \tilde{\mathbf{Q}} / \sqrt{d}$  // [N, m]
5: // Gather the top- $k$  activated key-value pairs
6:  $\mathcal{I}^{\text{kv}} = \text{Flatten}(\text{TopK}(\mathbf{S}^{\text{kv}\top}, k, \text{dim}=1))$  // [m*k]
7:  $\mathbf{K}^{\text{expt}}, \mathbf{V}^{\text{expt}} = \mathbf{K}[:, \mathcal{I}^{\text{kv}}], \mathbf{V}[:, \mathcal{I}^{\text{kv}}]$  // [d, m*k]
8: // Obtain landmark values (construct the shared expert)
9:  $\tilde{\mathbf{V}} = \mathbf{V} \text{softmax}(\mathbf{S}^{\text{kv}})$  // [d, m]
10: // Always route queries to the shared expert
11:  $\mathbf{O}^{\text{share}} = \text{FlashAttention}(\mathbf{Q}, \tilde{\mathbf{Q}}, \tilde{\mathbf{V}})$ 
12: // Sparsely route queries to other experts
13:  $\mathcal{I}^{\text{expt}} = \text{ArgSort}(\text{ArgMax}(\tilde{\mathbf{Q}}^\top \mathbf{Q}, \text{dim}=0))$  // [N]
14:  $\mathbf{O}^{\text{expt}} = \text{FlashAttention}(\mathbf{Q}[:, \mathcal{I}^{\text{expt}}], \mathbf{K}^{\text{expt}}, \mathbf{V}^{\text{expt}},$ 
    cu_seqlens_q=CumSum(BinCount( $\mathcal{I}^{\text{expt}}$ )),
    cu_seqlens_k=[0, k, 2k, ..., mk])
15: // Combine results via online softmax
16:  $\mathbf{O} = \text{Combine}(\mathbf{O}^{\text{share}}, \mathbf{O}^{\text{expt}})$  // [d, N]
17: return  $\mathbf{O}$ 
    
```

---

as a single standard attention, as shown in Fig. 2. Therefore, our **MiTA Attention** can be written as:

$$\text{MiTA}(\mathbf{q}) = \mathbf{V}^* \text{softmax}(\mathbf{K}^{*\top} \mathbf{q} / \sqrt{d}), \quad (10)$$

$$\mathbf{K}^* = [\tilde{\mathbf{Q}}, \mathbf{K}^{(e_1(\mathbf{q}))}, \dots, \mathbf{K}^{(e_s(\mathbf{q}))}], \quad (11)$$

$$\mathbf{V}^* = [\tilde{\mathbf{V}}, \mathbf{V}^{(e_1(\mathbf{q}))}, \dots, \mathbf{V}^{(e_s(\mathbf{q}))}], \quad (12)$$

where  $\mathbf{K}^*, \mathbf{V}^* \in \mathbb{R}^{d \times (m+ks)}$  are the key-value pairs that a query  $\mathbf{q}$  attends to in our MiTA, and  $s$  is the number of routed experts (not counting the shared expert) per query.<sup>2</sup>

Note that, in practice, the attention can still be computed expert-wise and then combined, thanks to the online softmax (Milakov & Gimelshein, 2018), as in the FlashAttention (Dao, 2024) implementation of Lu et al. (2025).

Our MiTA attention in Eq. (10) can be summarized as follows: a) obtain landmark queries  $\tilde{\mathbf{Q}}$  from queries  $\mathbf{Q}$  via average pooling; b) use landmark queries  $\tilde{\mathbf{Q}}$  to query keys  $\mathbf{K}$ , thereby i) constructing deformable fast-weight experts (i.e.,  $\mathbf{K}^{(i)}, \mathbf{V}^{(i)}$ ) via the top- $k$  activations and ii) extracting

<sup>2</sup> $m$  is the number of routed expert in total.



Figure 4. The token pruning effect of MiTA Attention. Each row visualizes, for each layer, the positions of key-value pairs (aggregated over heads) selected as experts; the leftmost image shows the original input. In later layers, most tokens are effectively “pruned” (i.e., not selected as experts), and attention concentrates on class-relevant regions. The examples are sampled from the ImageNet-1K training set.

landmark values  $\tilde{V}$  via cross-attention; c) route queries  $Q$  sparsely to the experts, while keeping the shared expert (i.e.,  $\tilde{Q}$ ,  $\tilde{V}$ ) always active.

**Implementations.** In particular, we implement our MiTA attention in Eq. (10) with  $s = 1$ , i.e., each query is dispatched to the shared expert and exactly one additional fast-weight expert. Algorithm 1 presents the pseudocode of our MiTA, which matches queries to experts by sorting queries according to their expert assignments  $e_1(q)$ . The more general but more complex case with  $s > 1$  can be implemented via MoBA (Lu et al., 2025).

**Complexity analysis.** The computational complexity of Eq. (10) alone is  $\mathcal{O}(N(m + ks))$ , whereas full attention incurs  $\mathcal{O}(N^2)$ ; in practice,  $N \gg m + ks$ . Moreover, the cross-attention operations in Eqs. (8) and (10) can be accelerated by the FlashAttention family (Dao et al., 2022; Dao, 2024; Shah et al., 2024). The primary bottleneck comes from the gather operation in Eq. (6): it entails irregular (random) memory access and is therefore likely to make the overall pipeline memory-bound. Nonetheless, Deepseek Sparse Attention suggests that this limitation can be mitigated via its optimized implementation (Liu et al., 2025, Fig. 3). Moreover, compared with prior top- $k$  attention (You et al., 2025; Liu et al., 2025), which instantiate a private fast-weight expert per query ( $N$  experts in total) without routing, our MiTA uses a *fixed* (yet tunable) number (i.e.,  $m$ ) of fast-weight experts, which is more hardware-friendly, at the cost of an  $N$ -to- $m$  routing step, which is explored in MoBA (Lu et al., 2025). In summary, our MiTA is composed of operations that have already been validated by engineering-centric prior work, allowing us to focus on the fast-weight scaling perspective, its taxonomy, the combination of the two scaling strategies, and the construction of a fixed number of deformable fast-weight experts.

### 3.3. Fit MiTA into the Fast-Weight Scaling Taxonomy

While MiTA is primarily motivated by combining the two complementary scaling strategies, we find that it also enriches the remaining dimensions of the fast-weight scaling

taxonomy proposed in Sec. 3.1. This subsection will briefly discuss each of them.

**Expert construction.** This core dimension determines the expert type and count, and hence the routing topology. An important consideration is what the construction conditions on: the query only (e.g., DAT (Xia et al., 2022)), the key-value pairs only (e.g., MHLA (Zhang et al., 2026)), or both. When using key-value pairs, the construction may be content-dependent and thus deformable (e.g., DSA (Liu et al., 2025)) or merely position-driven (e.g., MoBA (Lu et al., 2025)). While most efficient attention methods condition on one of the above aspects, our MiTA conditions on all of them by extracting landmark queries from queries and then probe the full key-value pool. We illustrate a resulting benefit of this design in Fig. 4.

**Expert type and count.** Expert types can be categorized in three classes: a) linear layers (e.g., linear attention), b) MLPs (e.g., sparse attention and PVT (Wang et al., 2021)), c) arbitrary modules (e.g., test-time training). The scaling-by-routing branch of MiTA is restricted to MLP experts, as in sparse attention. However, the scaling-by-compression branch can be implemented through test-time training, thereby generalizing to other modules. As for the expert count, MiTA controls it via the hyperparameter  $m$ . One benefit of this design has been discussed in complexity analysis. Another benefit is that it enables expert composition through the routing mechanism.

**Routing topology.** In MiTA, there is a fixed number of base sparse patterns (i.e., fast-weight experts), which is a substantial improvement over efficient attention with only a single expert, yet is still far fewer than prior top- $k$  attention (You et al., 2025; Liu et al., 2025), which has  $N$  experts. Crucially, to compensate for this limitation, MiTA can resort to the routing mechanism to compose these  $m$  base experts: when routing each query to  $s$  experts, the number of effective sparse patterns (i.e., the combinatorial number of experts) is  $\binom{m}{s}$ . In particular, when  $s = 1$ , routing may degenerate into clustering, restricting information flow within each cluster. We thus quantify the positional overlap be-

tween an expert’s gathered key–value pairs and the queries routed to it. As shown in Fig. 5, the overlap remains consistently modest across layers, suggesting that MiTA with  $s = 1$  performs routing rather than hard clustering.

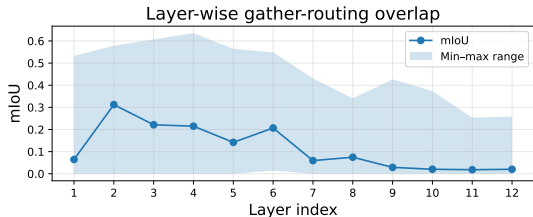


Figure 5. The layer-wise positional overlap (between the key–value pairs gathered by an expert and the queries routed to it) is quantified by mIoU, averaged over experts and attention heads.

## 4. Experiments

To verify the efficacy of our MiTA Attention, we conduct image classification experiments on ImageNet-1K (Deng et al., 2009) and semantic segmentation experiments on ADE20K (Zhou et al., 2019). Moreover, we assess the long sequence modeling capability of MiTA on the Long Range Arena benchmark (Tay et al., 2021), and report its wall-clock training/inference speed against full attention on extremely long sequences. Furthermore, we study the robustness (or generalization) of MiTA under varying expert count ( $m$ ) and width ( $k$ ) when the model is fixed after training. Additionally, we explore a broader problem of interest: the *algorithmic generalization* of Transformers across attention mechanisms.

### 4.1. Image Classification

Current advances in efficient attention on ImageNet-1K are typically accompanied by extra components such as depth-wise convolutions, which obscure the expressiveness gap between the proposed efficient mechanisms and full attention. To this end, we report a fair comparison in Tab. 2. Specifically, we train all models using the DeiT (Touvron et al., 2021) recipe and vary only the attention mechanism. Meanwhile, in Tab. 3, we compare our best-performing ViT variant based on MiTA Attention against state-of-the-art and efficient ViTs.

**Implementation details.** We use an image size of 224 with a patch size of 16, and set  $s = 1$ ,  $m = k = 25$  for MiTA Attention.<sup>3</sup> Under this setting, each query attends to  $m + ks = 50$  key-value pairs.

**Results.** As indicated in Tab. 2, without extra components, MiTA Attention outperforms other efficient attention by a substantial margin (at least 0.8% and up to 3.1%). Although

<sup>3</sup>We set  $s = 1$  throughout this work for a preliminary study. As analyzed in Sec. 3.3, this choice does not fully exploit the expressiveness of MiTA Attention.

Table 2. Results on ImageNet-1K training from scratch. <sup>Bias</sup>: using the agent bias (Han et al., 2024b); <sup>DWC</sup>: using depth-wise convolution; <sup>Gate</sup>: adding the attention output to the residual with data-dependent gating. PolaFormer (Meng et al., 2025), MHLA (Zhang et al., 2026), and FLatten (Han et al., 2023) are variants of linear attention. BRA (Zhu et al., 2023) and Agent Attention can be viewed as degenerate cases of MiTA attention, scaling by only routing and only compression, respectively.

Method	# Params	FLOPs	Acc. (%)
DeiT-T	5.7M	1.2G	72.2
Linear-DeiT-T	5.7M	1.1G	68.0
PolaFormer-DeiT-T	5.7M	1.2G	68.1
MHLA-DeiT-T	5.7M	1.1G	69.2
FLatten-DeiT-T	6.1M	1.1G	70.2
BRA-DeiT-T	5.7M	1.1G	70.2
Agent-DeiT-T	5.7M	1.1G	70.3
Agent-DeiT-T <sup>Bias</sup>	6.0M	1.2G	71.1
MiTA-DeiT-T	5.7M	1.1G	71.1 (-1.1)
MiTA-DeiT-T <sup>DWC</sup>	5.7M	1.1G	73.4 (+1.2)
DeiT-S	22M	4.6G	79.9
Agent-DeiT-S	22M	4.4G	78.5
Agent-DeiT-S <sup>Bias</sup>	23M	4.4G	79.1
MiTA-DeiT-S	22M	4.4G	79.8 (-0.1)
MiTA-DeiT-S <sup>DWC</sup>	22M	4.4G	80.6 (+0.7)
MiTA-DeiT-S <sup>DWC, Gate</sup>	22M	4.7G	81.2 (+1.3)

Table 3. Comparison with SOTA and efficient ViTs on ImageNet-1K. We compare against a recent state-of-the-art ViT variant, ViT-5 (Wang et al., 2026), as well as strong baselines such as DeiT and DeiT-III (Touvron et al., 2022). We also include efficient ViTs, including sparse models (SViTE (Chen et al., 2021a) and Sparsifiner (Wei et al., 2023)) and scaling-by-compression models (InLine (Han et al., 2024a) and Agent Attention).

Method	# Params	FLOPs	Acc. (%)
ViT-5-S	22M	4.7G	82.2
DeiT-S	22M	4.6G	79.9
DeiT-III-S	22M	4.6G	81.4
SViTE-S	11M	2.5G	79.7
Sparsifiner-S	23M	4.5G	79.9
InLine-DeiT-S	17M	5.0G	80.2
Agent-DeiT-S <sup>Bias, DWC</sup>	23M	4.4G	80.5
MHLA-DeiT-S <sup>DWC</sup>	22M	4.2G	81.0
MiTA-ViT-5-S	22M	4.5G	81.3 (-0.9)
MiTA-ViT-5-S <sup>DWC</sup>	22M	4.5G	81.7 (-0.5)

Agent Attention can narrow the gap by using agent bias<sup>4</sup>, it still underperforms MiTA Attention on small-sized models by 0.7%. Moreover, a severe limitation of this trick is that it is currently not supported by FlashAttention. As shown in Tab. 3, when equipped with the architectural modifications explored in ViT-5 (Wang et al., 2026), MiTA Attention outperforms a range of strong ViT baselines and approaches state-of-the-art performance within a small margin while using fewer FLOPs.

<sup>4</sup>An agent bias  $B \in \mathbb{R}^{N \times m}$  is added to attention scores as  $\text{softmax}(K^T Q + B)$ .

Table 4. Results on LRA benchmark. For each task, we report the accuracy and training throughput (steps/s), along with the average accuracy across tasks and the total training wall-clock time (hours). †: a route-only variant of MiTA Attention, where the number of entries attended per query kept unchanged by increasing  $k$ .

Method	ListOps (2K)	Text (4K)	Retrieval (4K)	Image (1K)	Pathfinder (1K)	Avg. / Tot.
Standard Attention	37.35 / 12.7	63.63 / 3.8	79.90 / 1.9	40.38 / 5.7	69.68 / 5.7	58.19 / 10.6
Reformer	18.55 / 34.1	65.08 / 16.8	78.77 / 8.5	44.04 / 8.3	69.04 / 8.5	55.10 / 4.5
Linformer	38.05 / 35.0	56.69 / 24.6	78.41 / 13.7	39.56 / 11.9	67.13 / 11.9	55.97 / 3.1
Performer	17.84 / 28.0	65.13 / 16.5	77.18 / 8.9	36.64 / 8.1	70.20 / 8.0	53.40 / 4.7
Nyströmformer	29.69 / 22.0	65.84 / 16.7	79.68 / 8.8	36.83 / 4.5	72.50 / 4.5	56.91 / 7.3
MiTA Attention†	37.20 / 25.4	64.09 / 22.2	79.92 / 13.1	40.17 / 5.3	72.66 / 6.3	58.81 / 5.5
MiTA Attention	37.20 / 52.5 ( $\times 4.1$ )	63.47 / 37.7 ( $\times 9.9$ )	79.88 / 19.6 ( $\times 10.3$ )	40.72 / 13.6 ( $\times 2.4$ )	73.26 / 15.3 ( $\times 2.7$ )	58.91 / 2.4 ( $\downarrow 77\%$ )

Table 5. Results on ADE20K semantic segmentation.  $\nabla$ : the attention mechanism is directly replaced, rather than being natively pre-trained. Mask Transformer is the decoder introduced in the pioneering work Segmenter (Strudel et al., 2021) for Transformer-based segmentation, while DEPICT (Wen & Li, 2024) and CBT (Wen et al., 2025) are two principled improvements upon it.

Backbone	Seg. head	Resolution	FLOPs	mIoU (%)
ViT-T	Mask Trans.	512 <sup>2</sup>	13G	38.1
ViT-T	DEPICT	512 <sup>2</sup>	13G	39.3
ViT-T	CBT	512 <sup>2</sup>	12G	39.1
MiTA-ViT-T $\nabla$	CBT	512 <sup>2</sup>	7G ( $\downarrow 42\%$ )	36.5 ( $-2.6$ )
ViT-S	Mask Trans.	512 <sup>2</sup>	38G	45.3
ViT-S	DEPICT	512 <sup>2</sup>	35G	46.7
ViT-S	CBT	512 <sup>2</sup>	33G	45.8
MiTA-ViT-S $\nabla$	CBT	512 <sup>2</sup>	25G ( $\downarrow 24\%$ )	44.5 ( $-1.3$ )
ViT-B	Mask Trans.	512 <sup>2</sup>	128G	48.5
ViT-B	DEPICT	512 <sup>2</sup>	111G	49.2
ViT-B	CBT	512 <sup>2</sup>	111G	49.3
MiTA-ViT-B $\nabla$	CBT	512 <sup>2</sup>	95G ( $\downarrow 14\%$ )	48.1 ( $-1.2$ )
ViT-L	Mask Trans.	640 <sup>2</sup>	667G	51.8
ViT-L	DEPICT	640 <sup>2</sup>	628G	52.9
ViT-L	CBT	640 <sup>2</sup>	622G	53.3
MiTA-ViT-L $\nabla$	CBT	640 <sup>2</sup>	508G ( $\downarrow 18\%$ )	50.5 ( $-2.8$ )

## 4.2. Semantic Segmentation

ADE20K (Zhou et al., 2019) is a scene-centric dataset for semantic segmentation, which requires higher image resolutions to preserve fine-grained details such as object boundaries. In Tab. 5, we apply MiTA Attention to the backbone for efficient visual encoding and compare against methods with ViT backbones and Transformer-based segmentation heads.

**Implementation details.** ViT backbones (Steiner et al., 2022) are pretrained on ImageNet-21K with an image size of 384 and a patch size of 16. We use a consistent patch size of 16 when training on ADE20K, and set  $s = 1$ ,  $m = k = 49$  for MiTA Attention. Under this setting, each query attends to  $m + ks = 98$  key-value pairs, while it is 1,024 (for 512<sup>2</sup> image resolution) or 1,600 (640<sup>2</sup> resolution) in full attention.

Table 6. Finetuning results. We finetune ImageNet-21K pretrained ViTs (Steiner et al., 2022) on ImageNet-1K, replacing the standard attention with Agent Attention or MiTA Attention. †: the number of agent tokens (i.e., landmark queries) is increased from 49 (default) to 64.

Method	Tiny	Small	Base	Large
Standard Attention	76.9	81.2	84.4	85.9
Linear Attention	73.2	78.6	79.8	80.7
Agent Attention	74.6	79.7	81.4	83.5
Agent Attention†	74.7	79.9	81.5	83.8
MiTA Attention	75.6 ( $-1.3$ )	80.9 ( $-0.3$ )	82.8 ( $-1.6$ )	85.5 ( $-0.4$ )

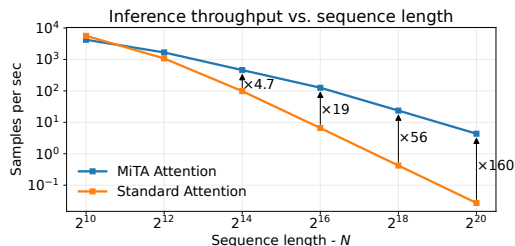


Figure 6. Inference throughput. The results are measured on a three-layer Transformer with an embedding dimension of 128, and the batch size is tuned for each run to maximize throughput.

**Results.** As depicted in Tab. 5, MiTA Attention remarkably reduces the FLOPs (by up to 42%) while achieving comparable segmentation performance. Note that MiTA Attention is not fully exploited here because the backbone is not natively pretrained with it.

## 4.3. Evaluation on Long Sequences

As a preliminary validation for long-sequence modeling, we evaluate MiTA Attention on the Long Range Arena (LRA) benchmark (Tay et al., 2021) and compare against several classical efficient attention methods (Kitaev et al., 2020; Wang et al., 2020; Choromanski et al., 2021; Xiong et al., 2021). We report their accuracy and training throughput (and wall-clock time) on LRA in Tab. 4, while the inference throughput improvement of MiTA Attention over standard attention is shown in Fig. 6.

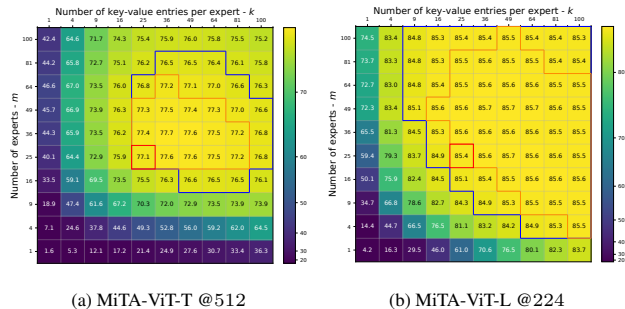


Figure 7. MiTA Attention’s generalization across  $m$  and  $k$ . The red box marks the training (or finetuning) ( $m, k$ ) and the corresponding baseline accuracy on ImageNet-1K. The orange boundary marks the inference ( $m, k$ ) configurations that exceed the baseline accuracy, and the blue boundary marks those achieve 99% of the baseline accuracy. Best viewed when zoomed in.

**Implementation details.** The training configuration follows Xiong et al. (2021) and hyperparameters are kept consistent across all methods for a fair comparison. Thus, the reported accuracies are not tuned to fully exploit the best performance of each approach. We set  $s = 1$  and  $m = k = 256$  for MiTA Attention. Throughput and wall-clock time reported in Tab. 4 and Fig. 6 are measured on a 24GB RTX 4090. Standard attention is implemented with PyTorch’s fused kernel (i.e., FlashAttention).

**Results.** As shown in Tab. 4, MiTA Attention achieves accuracy comparable to standard attention, while providing a substantial speedup that reduces total training time by 77%. Notably, the route-only variant of MiTA Attention also performs well but is slower, since gathering more key-value pairs incurs higher overhead. This suggest that using a shared, compressed set of key-value pairs can effectively represent thousands of routed original pairs.

#### 4.4. Algorithmic Generalization

Broadly, generalization typically refers to performance beyond the training data, e.g., from the training set to the validation set, length extrapolation (Zhao et al., 2024) (from the training resolution to a new one). Motivated by the unifying perspective for efficient attention, this work investigate a new dimension of generalization: *algorithmic generalization*, i.e., performance beyond the training algorithm (e.g., attention mechanism).

In Fig. 7, we study MiTA Attention’s generalization across hyperparameters: the expert count  $m$  and expert width  $k$ . Note that changing an algorithm’s hyperparameters is analogous to changing the input resolution. Moreover, in Fig. 8, we study how an attention mechanism generalizes to others. Specifically, given a model trained with one attention mechanism (*training attention*), we replace it with a different mechanism (*inference attention*) at test time. Beyond the

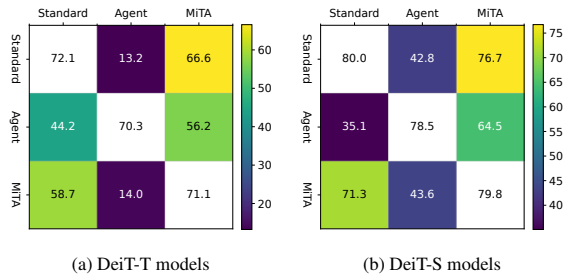


Figure 8. Evaluation with a different inference attention. The x-axis indexes the training attention, while the y-axis indexes the inference attention. We omit the diagonal entries from the heatmap since they are not of interest. Currently, only standard attention, Agent Attention, and MiTA Attention are included.

generalization setting, where model parameters are fixed, we also finetune models pretrained on a large-scale dataset with a different *finetuning attention* in Tab. 6.

**Implementation details.** ViTs (Steiner et al., 2022) in Tab. 5 are pretrained on ImageNet-21K with an image size of 224 and a patch size of 16. We finetune them for 50 epochs with the AdamW optimizer, using the listed attention mechanisms (including standard attention). The model in Fig. 7(a) is similarly finetuned, but starts from a ViT pretrained with an image size of 384. Models in Fig. 8 are the same as those in Tab. 2.

**Results.** Fig. 7 suggests that MiTA Attention generalizes well when scaling up the expert count and width: many configurations exceeds the original result. This indicates a promising strategy: train MiTA Attention with smaller  $m$  and  $k$  for efficiency, then increase  $m$  or  $k$  at inference to obtain gains. In Fig. 8, we observe that standard attention and MiTA Attention generalize to each other better than other pairs, especially when training with standard attention and testing with MiTA Attention, which retains over 95% of the original performance with linear complexity. Regarding finetuning, Tab. 6 shows that parameters pretrained with standard attention transfer more easily to MiTA Attention, while Agent Attention struggles to narrow this gap even when increasing the number of agent tokens.

## 5. Conclusion

We adopted fast-weight scaling as a unifying viewpoint for efficient attention and introduced a five-dimensional taxonomy. Moreover, we proposed a novel efficient attention method, which is termed as MiTA Attention, to bridge the two scaling strategies—scaling by routing and scaling by compression—and construct a tunable number of deformable fast-weight experts. We provided a detailed analysis of both the taxonomy and our MiTA Attention, suggesting a principled and promising path for developing efficient attention from the fast-weight scaling perspective.

## Broader Impact

This paper presents work whose goal is to advance the field of Machine Learning. There are many potential societal consequences of our work, none of which we feel must be specifically highlighted here.

## References

- Ba, J. and Caruana, R. Do deep nets really need to be deep? In *NeurIPS*, 2014.
- Behrouz, A., Zhong, P., and Mirrokni, V. Titans: Learning to memorize at test time. *arXiv preprint arXiv:2501.00663*, 2024.
- Beltagy, I., Peters, M. E., and Cohan, A. Longformer: The long-document transformer. *arXiv preprint arXiv:2004.05150*, 2020.
- Bietti, A., Cabannes, V., Bouchacourt, D., Jégou, H., and Bottou, L. Birth of a transformer: A memory viewpoint. In *NeurIPS*, 2023.
- Cai, S., Yang, C., Zhang, L., Guo, Y., Xiao, J., Yang, Z., Xu, Y., Yang, Z., Yuille, A., Guibas, L., et al. Mixture of contexts for long video generation. *arXiv preprint arXiv:2508.21058*, 2025.
- Carion, N., Massa, F., Synnaeve, G., Usunier, N., Kirillov, A., and Zagoruyko, S. End-to-end object detection with transformers. In *ECCV*, 2020.
- Chan, S. C. Y., Santoro, A., Lampinen, A. K., Wang, J. X., Singh, A. K., Richemond, P. H., McClelland, J. L., and Hill, F. Data distributional properties drive emergent in-context learning in transformers. In *NeurIPS*, 2022.
- Chen, T., Cheng, Y., Gan, Z., Yuan, L., Zhang, L., and Wang, Z. Chasing sparsity in vision transformers: An end-to-end exploration. In *NeurIPS*, 2021a.
- Chen, Z., Zhu, Y., Zhao, C., Hu, G., Zeng, W., Wang, J., and Tang, M. DPT: Deformable patch-based transformer for visual recognition. In *ACMMM*, 2021b.
- Cheng, B., Schwing, A., and Kirillov, A. Per-pixel classification is not all you need for semantic segmentation. In *NeurIPS*, 2021.
- Cheng, H., Zhang, M., and Shi, J. Q. A survey on deep neural network pruning: Taxonomy, comparison, analysis, and recommendations. *TPAMI*, 46(12):10558–10578, 2024.
- Choromanski, K. M., Likhoshesterov, V., Dohan, D., Song, X., Gane, A., Sarlós, T., Hawkins, P., Davis, J. Q., Mohiuddin, A., Kaiser, L., Belanger, D. B., Colwell, L. J., and Weller, A. Rethinking attention with performers. In *ICLR*, 2021.
- Dai, D., Deng, C., Zhao, C., Xu, R. X., Gao, H., Chen, D., Li, J., Zeng, W., Yu, X., Wu, Y., Xie, Z., Li, Y. K., Huang, P., Luo, F., Ruan, C., Sui, Z., and Liang, W. DeepSeekMoE: Towards ultimate expert specialization in mixture-of-experts language models. In *ACL*, 2024.
- Dai, J., Qi, H., Xiong, Y., Li, Y., Zhang, G., Hu, H., and Wei, Y. Deformable convolutional networks. In *ICCV*, 2017.
- Dao, T. FlashAttention-2: Faster attention with better parallelism and work partitioning. In *ICLR*, 2024.
- Dao, T., Fu, D., Ermon, S., Rudra, A., and Ré, C. FlashAttention: Fast and memory-efficient exact attention with IO-awareness. *NeurIPS*, 2022.
- Darcet, T., Oquab, M., Mairal, J., and Bojanowski, P. Vision transformers need registers. In *ICLR*, 2024.
- Deng, J., Dong, W., Socher, R., Li, L., Li, K., and Fei-Fei, L. ImageNet: A large-scale hierarchical image database. In *CVPR*, 2009.
- Dong, X., Bao, J., Chen, D., Zhang, W., Yu, N., Yuan, L., Chen, D., and Guo, B. CSWin transformer: A general vision transformer backbone with cross-shaped windows. In *CVPR*, 2022.
- Dosovitskiy, A., Beyer, L., Kolesnikov, A., Weissenborn, D., Zhai, X., Unterthiner, T., Dehghani, M., Minderer, M., Heigold, G., Gelly, S., Uszkoreit, J., and Housley, N. An image is worth 16x16 words: Transformers for image recognition at scale. In *ICLR*, 2021.
- Geva, M., Schuster, R., Berant, J., and Levy, O. Transformer feed-forward layers are key-value memories. In *EMNLP*, 2021.
- Han, D., Pan, X., Han, Y., Song, S., and Huang, G. FFlatten transformer: Vision transformer using focused linear attention. In *ICCV*, 2023.
- Han, D., Pu, Y., Xia, Z., Han, Y., Pan, X., Li, X., Lu, J., Song, S., and Huang, G. Bridging the divide: Reconsidering softmax and linear attention. In *NeurIPS*, 2024a.
- Han, D., Ye, T., Han, Y., Xia, Z., Pan, S., Wan, P., Song, S., and Huang, G. Agent attention: On the integration of softmax and linear attention. In *ECCV*, 2024b.
- Han, D., Li, Y., Li, T., Cao, Z., Wang, Z., Song, J., Cheng, Y., Zheng, B., and Huang, G. ViT<sup>3</sup>: Unlocking test-time training in vision. *arXiv preprint arXiv:2512.01643*, 2025.
- Hinton, G., Vinyals, O., and Dean, J. Distilling the knowledge in a neural network. *arXiv preprint arXiv:1503.02531*, 2015.
- Jia, W., Lu, Y., Huang, M., Wang, H., Huang, B., Chen, N., Liu, M., Jiang, J., and Mao, Z. MoGA: Mixture-of-groups attention for end-to-end long video generation. *arXiv preprint arXiv:2510.18692*, 2025.
- Jiang, H., Li, Y., Zhang, C., Wu, Q., Luo, X., Ahn, S., Han, Z., Abdi, A. H., Li, D., Lin, C., Yang, Y., and Qiu, L. MInference 1.0: Accelerating pre-filling for long-context LLMs via dynamic sparse attention. In *NeurIPS*, 2024.
- Kaplan, J., McCandlish, S., Henighan, T., Brown, T. B., Chess, B., Child, R., Gray, S., Radford, A., Wu, J., and Amodei, D. Scaling laws for neural language models. *arXiv preprint arXiv:2001.08361*, 2020.
- Katharopoulos, A., Vyas, A., Pappas, N., and Fleuret, F. Transformers are RNNs: Fast autoregressive transformers with linear attention. In *ICML*, 2020.
- Kirsch, L., Harrison, J., Sohl-Dickstein, J., and Metz, L. General-purpose in-context learning by meta-learning transformers. *arXiv preprint arXiv:2212.04458*, 2022.
- Kitaev, N., Kaiser, L., and Levskaya, A. Reformer: The efficient transformer. In *ICLR*, 2020.

- Lai, X., Lu, J., Luo, Y., Ma, Y., and Zhou, X. FlexPrefix: A context-aware sparse attention mechanism for efficient long-sequence inference. In *ICLR*, 2025.
- Liu, A., Mei, A., Lin, B., Xue, B., Wang, B., Xu, B., Wu, B., Zhang, B., Lin, C., Dong, C., et al. DeepSeek-v3. 2: Pushing the frontier of open large language models. *arXiv preprint arXiv:2512.02556*, 2025.
- Lu, E., Jiang, Z., Liu, J., Du, Y., Jiang, T., Hong, C., Liu, S., He, W., Yuan, E., Wang, Y., et al. MoBA: Mixture of block attention for long-context llms. *arXiv preprint arXiv:2502.13189*, 2025.
- Meng, W., Luo, Y., Li, X., Jiang, D., and Zhang, Z. PolaFormer: Polarity-aware linear attention for vision transformers. In *ICLR*, 2025.
- Milakov, M. and Gimelshein, N. Online normalizer calculation for softmax. *arXiv preprint arXiv:1805.02867*, 2018.
- Riquelme, C., Puigcerver, J., Mustafa, B., Neumann, M., Jenatton, R., Pinto, A. S., Keysers, D., and Houlsby, N. Scaling vision with sparse mixture of experts. In *NeurIPS*, 2021.
- Roy, A., Saffar, M., Vaswani, A., and Grangier, D. Efficient content-based sparse attention with routing transformers. *TACL*, 9:53–68, 2021.
- Schlag, I., Irie, K., and Schmidhuber, J. Linear transformers are secretly fast weight programmers. In *ICML*, 2021.
- Schmidhuber, J. Learning to control fast-weight memories: An alternative to dynamic recurrent networks. *Neural Computation*, 4(1):131–139, 1992.
- Shah, J., Bikshandi, G., Zhang, Y., Thakkar, V., Ramani, P., and Dao, T. FlashAttention-3: Fast and accurate attention with asynchrony and low-precision. In *NeurIPS*, 2024.
- Steiner, A. P., Kolesnikov, A., Zhai, X., Wightman, R., Uszkoreit, J., and Beyer, L. How to train your ViT? Data, augmentation, and regularization in vision transformers. *TMLR*, 2022.
- Strudel, R., Garcia, R., Laptev, I., and Schmid, C. Segmenter: Transformer for semantic segmentation. In *ICCV*, 2021.
- Sun, Y., Li, X., Dalal, K., Xu, J., Vikram, A., Zhang, G., Dubois, Y., Chen, X., Wang, X., Koyejo, S., Hashimoto, T., and Guestrin, C. Learning to (learn at test time): RNNs with expressive hidden states. In *ICML*, 2025.
- Tan, M. and Le, Q. EfficientNet: Rethinking model scaling for convolutional neural networks. In *ICML*, 2019.
- Tay, Y., Dehghani, M., Abnar, S., Shen, Y., Bahri, D., Pham, P., Rao, J., Yang, L., Ruder, S., and Metzler, D. Long range arena: A benchmark for efficient transformers. In *ICLR*, 2021.
- Touvron, H., Cord, M., Douze, M., Massa, F., Sablayrolles, A., and Jégou, H. Training data-efficient image transformers & distillation through attention. In *ICML*, 2021.
- Touvron, H., Cord, M., and Jégou, H. DeiT III: Revenge of the ViT. In *ECCV*, 2022.
- Vaswani, A., Shazeer, N., Parmar, N., Uszkoreit, J., Jones, L., Gomez, A. N., Kaiser, Ł., and Polosukhin, I. Attention is all you need. *NeurIPS*, 2017.
- Wang, F., Ren, S., Zhang, T., Neskovic, P., Bhattad, A., Xie, C., and Yuille, A. ViT-5: Vision transformers for the mid-2020s. *arXiv preprint arXiv:2602.08071*, 2026.
- Wang, S., Li, B. Z., Khabsa, M., Fang, H., and Ma, H. Linformer: Self-attention with linear complexity. *arXiv preprint arXiv:2006.04768*, 2020.
- Wang, W., Xie, E., Li, X., Fan, D., Song, K., Liang, D., Lu, T., Luo, P., and Shao, L. Pyramid vision transformer: A versatile backbone for dense prediction without convolutions. In *ICCV*, 2021.
- Wei, C., Duke, B., Jiang, R., Aarabi, P., Taylor, G. W., and Shkurti, F. Sparsifiner: Learning sparse instance-dependent attention for efficient vision transformers. In *CVPR*, 2023.
- Wen, Q. and Li, C.-G. Rethinking decoders for transformer-based semantic segmentation: A compression perspective. In *NeurIPS*, 2024.
- Wen, Q., Huang, Z., and Li, C.-G. Towards interpretable and efficient attention: Compressing all by contracting a few. In *NeurIPS*, 2025.
- Wu, B., Chen, M., Luo, X., Yan, S., Yu, Q., Xia, F., Zhang, T., Zhan, H., Zhong, Z., Zhou, X., et al. Parallel loop transformer for efficient test-time computation scaling. *arXiv preprint arXiv:2510.24824*, 2025a.
- Wu, J., Hou, L., Yang, H., Tao, X., Tian, Y., Wan, P., Zhang, D., and Tong, Y. VMoBA: Mixture-of-block attention for video diffusion models. *arXiv preprint arXiv:2506.23858*, 2025b.
- Xia, Z., Pan, X., Song, S., Li, L. E., and Huang, G. Vision transformer with deformable attention. In *CVPR*, 2022.
- Xiong, Y., Zeng, Z., Chakraborty, R., Tan, M., Fung, G., Li, Y., and Singh, V. Nyströmformer: A nyström-based algorithm for approximating self-attention. In *AAAI*, 2021.
- You, C., Wu, K., Jia, Z., Chen, L., Bhojanapalli, S., Guo, J., Evci, U., Wassenberg, J., Netrapalli, P., Willcock, J. J., et al. Spark transformer: Reactivating sparsity in FFN and attention. In *NeurIPS*, 2025.
- Yu, Q., Weber, M., Deng, X., Shen, X., Cremers, D., and Chen, L.-C. An image is worth 32 tokens for reconstruction and generation. In *NeurIPS*, 2024.
- Yuan, J., Gao, H., Dai, D., Luo, J., Zhao, L., Zhang, Z., Xie, Z., Wei, Y., Wang, L., Xiao, Z., et al. Native sparse attention: Hardware-aligned and natively trainable sparse attention. In *ACL*, 2025.
- Zhang, J., Su, R., Liu, C., Wei, J., Wang, Z., Zhang, P., Wang, H., Jiang, H., Huang, H., Xiang, C., Xi, H., Yang, S., Li, X., Hu, Y., Fu, T., Zhao, T., Zhang, Y., Jiang, Y., Chen, C., Jiang, K., Chen, H., Zhao, M., Xu, X., Zhu, J., and Chen, J. A survey of efficient attention methods: Hardware-efficient, sparse, compact, and linear attention. 2025.
- Zhang, K., Huang, Y., Deng, Y., Yu, J., Chen, J., Ling, H., Xie, E., and Zhou, D. MHLA: Restoring expressivity of linear attention via token-level multi-head. *arXiv preprint arXiv:2601.07832*, 2026.

Zhao, L., Feng, X., Feng, X., Zhong, W., Xu, D., Yang, Q., Liu, H., Qin, B., and Liu, T. Length extrapolation of transformers: A survey from the perspective of positional encoding. In *EMNLP*, 2024.

Zhou, B., Zhao, H., Puig, X., Xiao, T., Fidler, S., Barriuso, A., and Torralba, A. Semantic understanding of scenes through the ade20k dataset. *IJCV*, 127(3):302–321, 2019.

Zhu, L., Wang, X., Ke, Z., Zhang, W., and Lau, R. W. H. BiFormer: Vision transformer with bi-level routing attention. In *CVPR*, 2023.

Zhu, X., Su, W., Lu, L., Li, B., Wang, X., and Dai, J. Deformable DETR: Deformable transformers for end-to-end object detection. In *ICLR*, 2021.